

Granular mixing and segregation in zigzag chute flow

Suman K. Hajra, Deliang Shi, and J. J. McCarthy*

Department of Chemical and Petroleum Engineering, University of Pittsburgh, Pittsburgh, Pennsylvania 15261 USA

(Received 31 January 2012; revised manuscript received 12 October 2012; published 26 December 2012)

Periodic flow inversions have been shown as an effective means to eliminate both density (D system) and size (S system) segregation. The frequency of these inversions, however, is the key to applying this technique and is directly related to the inverse of the characteristic time of segregation. In this work, we study size segregation (S system) and adapt a size segregation model to compliment existing work on density segregation and, ultimately, aid in determining the critical forcing frequency for S systems. We determine the impact on mixing and segregation of both the binary size ratio and the length of each leg of a “zigzag chute”. Mixing is observed when $L < \bar{U}t_s$, where L , \bar{U} , and t_s denote the length of each leg of the zigzag chute, the average streamwise flow velocity of the particle, and the characteristic time of segregation, respectively.

DOI: [10.1103/PhysRevE.86.061318](https://doi.org/10.1103/PhysRevE.86.061318)

PACS number(s): 45.70.Mg

I. INTRODUCTION

Granular materials are widely used in industries such as cement, fertilizers, pharmaceuticals, construction, mining, and agriculture. These materials are often multicomponent and exhibit differences in size, density, shape, and roughness. In fact, even “pure” materials almost invariably exhibit a non-trivial size distribution. These materials, therefore, typically segregate, or demix, if they are subjected to flow or external agitation in the presence of a gravitational field. Moreover, even previously well-mixed particles will tend to segregate as they are transported from one place to another through a chute or conveyor, for example.

Segregation has been observed in most flows of granular mixtures, including granular convection [1], heap flows [2–5], and flows in rotating drums [6–8], to name a few. Despite this ubiquity, our understanding of segregation in even the simplest cases is incomplete, resulting in engineering approaches to the mixing of granular materials that are developed on an *ad hoc* basis and scale-up that is largely empirical.

Recently, a number of advances in segregation control and reduction have been reported in the literature. Samadani and Kudrolli [4] found that segregation could be reduced by adding a small volume fraction of fluid to different-sized particles. Similarly, Li and McCarthy [9] found that segregation could be turned on or off by adding a small amount of moisture to mixtures of particles with different sizes, densities, and/or surface characteristics. Jain *et al.* [10], and Thomas [11], performed experiments for binary mixtures composed of different-sized and different-density particles and they found that limited success in achieving mixing can be obtained if the denser beads are bigger and also if the ratio of particles size is greater than the ratio of particle density (sometimes requiring extreme ratios). Hajra and Khakhar [12] found that segregation could be eliminated by using a small rotating impeller placed at the axis of rotation, where the size of the impeller is very small when compared to the diameter of the cylinder.

In a complementary approach, Shi *et al.* [13] proposed to adapt a fluid-mixing technique—specifically, the use of periodic flow perturbations—to thwart segregation in a

material-independent way. In particular, they showed that periodic flow *inversions* either manually (in a chute) or via selective baffle placement (in tumbler-type mixer) can serve as a general method for eliminating segregation in free-surface flows for either density-driven (D systems) or size-driven (S systems) segregation. In their work, a simple model of D-system segregation was used to predict the required critical perturbation frequency as a function of shear rate and density ratio that matched experiment and computational (DEM simulation) results reasonably well.

In this work, we propose a model similar to that of Shi *et al.* [13] based on a segregation velocity expression that can be used to derive a critical frequency prediction for S-system segregation (as opposed to D systems). A range of experiments and DEM simulations are carried out to validate the critical forcing frequency model.

II. BACKGROUND

Density segregation is often thought to arise due to an effective “buoyant force” experienced by the particles [14,15]. Lighter particles may be considered to be immersed in an effective medium of higher density corresponding to the average density of the mixture, and heavier particles in a lower density effective media.

Size segregation, on the other hand, is considerably more difficult to model and strongly depends on the flow regime—i.e., dense versus dilute. Many works that focus on dilute or moderately dense flows adopt a kinetic theory-based approach. For example, Jenkins and Mancini [16] used a revised Enskog theory to develop a kinetic theory model for binary mixtures of smooth, nearly elastic spheres. They suggested that size segregation is due to granular thermal diffusion. Similarly, Hsiao and Hunt [17] considered the shear flow of a binary mixture of different-sized particles and showed that temperature-induced segregation can lead to the smaller particles migrating to the regions of higher granular temperature (irrespective of location) and is largely influenced by the “regime” of the flow (i.e., dilute versus dense flow). Recent work by Fan and Hill [18] experimentally confirmed that the sense of size segregation can vary, based on the flow regime examined. In work on dense flows in a chute, like those examined here, Savage and Lun [19] proposed a size

*jjmcc@pitt.edu

segregation model using a percolation argument. In short, percolation can be understood in the following way. When particles flow together in a dense flowing layer, small voids are more likely to be formed than larger ones. Thus, small particles move downward by dropping into the voids, and consequently, the large particles travel upward. Finally, using a phenomenological approach, Dolgunin and Ukolov [15] proposed a model for size and density segregation that depends on particle concentration and granular temperature.

While no unique model for segregation due to differences in size has been established, the phenomenological impact of the segregation is well known: for dense flows at reasonably low values of the granular temperature (i.e., those exhibited by the rolling regime of a tumbler mixer or in a nonaccelerating chute flow) small particles sink to the bottom of a flowing layer, while larger particles rise to the top. Coupled with the original observation based on D systems—that is, that more dense particles sink to the bottom of a flowing layer while lighter particles rise to the top—we can argue that, at least for rolling-regime tumblers and non-freely-accelerating chute flows, segregation has a preferred direction. This observation, along with the fact that segregation requires a finite time to reach fruition, means that one can determine the critical perturbation frequency required to thwart segregation (either in D systems, S Systems, or mixed-mode systems) simply by establishing a model of the segregation kinetics. In the next section, we outline just such a model for S systems, based in part on the work reviewed here, and then subsequently test it for S systems both computationally and experimentally. It is critical to point out here that the details and accuracy of this model may be limited (for example, granular temperature is included only indirectly via fitting parameters); however, the generic approach of perturbing a segregating flow above a critical forcing frequency (that can theoretically be tied to the segregation velocity) will be applicable to general granular flows and the details of the model can be enhanced as our understanding of segregation kinetics improves.

III. MATHEMATICAL MODEL

Taking the mass concentration of the smaller (i.e., the “segregating”) particles in a flow to be denoted as ϕ_1 and that of the larger particles to be ϕ_2 , we can define the mass fraction of the smaller particles to be $c = \phi_1/(\phi_1 + \phi_2)$. The variation of c in a flowing layer is then governed by a convective diffusion equation as

$$\frac{\partial c}{\partial t} + v_x \frac{\partial c}{\partial x} + v_y \frac{\partial c}{\partial y} = \frac{\partial}{\partial y} \left(D \frac{\partial c}{\partial y} - J_s \right), \quad (1)$$

when we neglect the diffusion and segregation fluxes in the flow direction (x). The first term on the right-hand side is the diffusional flux with D being the diffusion coefficient, while J_s represents the segregating flux. As noted above, previous researchers have come up with expressions for segregation due to differences in particle sizes [19] and mixed-size and density variation [15,20] that have taken similar form to that of Khakhar *et al.* [14]. We propose, therefore, a size segregation velocity from the following argument. If we assume that the segregation velocity is proportional to the difference between the small and segregating particle diameter and the average

diameter, we get

$$v_s = -K(d_1 - \langle d \rangle), \quad (2)$$

where $\langle d \rangle = \frac{d_1\phi_1 + d_2\phi_2}{\phi_1 + \phi_2}$ is the mass-averaged particle size, d_1 and d_2 are the diameter of small and large particles, respectively, and K is a constant to be discussed below. Expanding $\langle d \rangle$ and simplifying yields

$$v_s = -Kd_2(1 - c)(\bar{d} - 1), \quad (3)$$

where $\bar{d} = d_1/d_2$ is the size ratio. Finally, assuming that the constant K has both an intrinsic and a concentration-dependent component (K_T and K_S , respectively) that can be considered complex functions of granular temperature, local void fraction, gravity, particle sizes, density, shape, roughness, coefficient of friction, coefficient of restitution, etc., we get

$$v_s = [K_T + (1 - c)K_S](1 - c)(1 - \bar{d}). \quad (4)$$

Here, the parameters, K_T and K_S , will be considered fitting constants that will be obtained on a case-by-case experimental and computational basis. Using Eq. (4), we can obtain a segregation flux of the segregating species as

$$J_s = v_s c. \quad (5)$$

By substituting for v_s from Eq. (4), we get

$$J_s = [K_T + (1 - c)K_S](1 - \bar{d})c(1 - c). \quad (6)$$

We should note that when $\bar{d} = 1$ we recover $v_s = 0$ and $J_s = 0$. Similarly, concentration values of $c = 0$ or $c = 1$ lead to $J_s = 0$. A final point to be made at this time is that while a value of $c = 1$ leads to a v_s of zero, the segregation velocity actually *increases* as c approaches zero. This makes physical sense because the most rapid segregation should happen when one small particle trickles through a bed of large beads (although, obviously, when c is identically zero this analysis becomes meaningless).

Substituting the expression for the segregation flux J_s using Eq. (6) into our original convection-diffusion equation we obtain

$$\begin{aligned} \frac{\partial c}{\partial t} + v_x \frac{\partial c}{\partial x} + v_y \frac{\partial c}{\partial y} \\ = \frac{\partial}{\partial y} \left[D \frac{\partial c}{\partial y} - (K_T + (1 - c)K_S)(1 - \bar{d})c(1 - c) \right]. \end{aligned} \quad (7)$$

The focus of our present work is to establish the characteristic segregation time, which is inversely proportional to the critical forcing frequency that could be applied to eliminate size segregation. Here we discuss the approach to derive the critical perturbation frequency. The key to adapting this approach in order to eliminate free-surface segregation lies in recognizing that it takes a finite time for material to segregate and that there is always a preferred direction that particles tend to segregate. In order to exploit these two facts, one needs to perturb the flow at a sufficiently high frequency, f , such that $f > t_s^{-1}$, where t_s is the characteristic segregation time.

Using the model outlined above, the characteristic segregation time may then be written as

$$t_s = R_1 / [(K_T + (1 - c)K_S)(1 - c)(1 - \bar{d})], \quad (8)$$

where R_1 is the radius of the small particles. Now, using this value, we can define a segregation-based Peclet number by

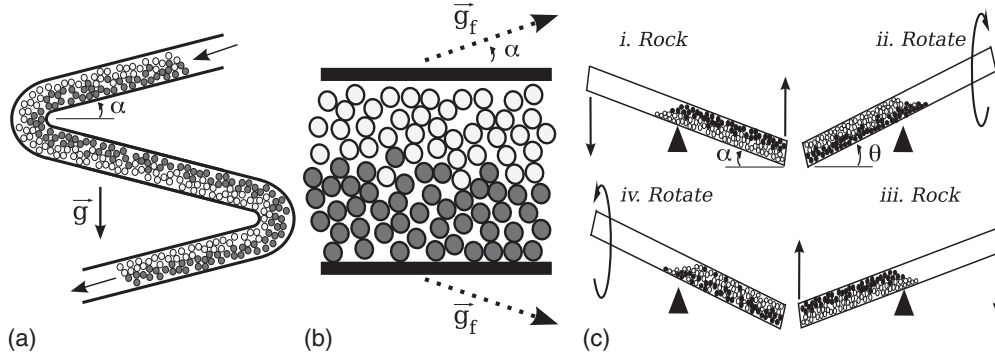


FIG. 1. A schematic representation of the (a) zigzag chute thought experiment, along with (b) the model simulation and (c) the experiment used to approximate it. (a) In a vertical gravity field, the chute changes direction periodically so that the material becomes roughly inverted. (b) In our simulations, we use a simple model of this, whereby the system is periodic in the flow direction and the inclined gravitational field, \vec{g}_f , has an oscillatory y component. (c) Experimentally, we put particles in a square tube, which is first rocked, then rotated in order to alter the sense of gravity [taking advantage of particles' tendency to behave like a solid during the rotate step by angling the tube at $\theta \gg \alpha$ (repose angle) during the rotate step].

defining a diffusion time scale as R_1^2/D , so that we get

$$\text{Pe} = \frac{(K_T + (1-c)K_S)(1-c)(1-\bar{d})R_1}{D}, \quad (9)$$

where D is the collisional diffusivity. Because of the current theoretical uncertainty and the time-varying nature of our flow (as well as our granular temperature, local void fraction, system nonuniformity, etc.), we treat $\beta = K_T R_1/D$ and $\alpha = K_S R_1/D$ as fitting parameters that should be a decreasing function of fluctuation energy of the flow and should be close to unity at small to moderate energies. This yields

$$\text{Pe} = [\beta + (1-c)\alpha](1-c)(1-\bar{d}). \quad (10)$$

Finally, the particle diffusivity in sheared granular flows was obtained by Savage [21] from numerical simulations of shear flow of nearly elastic hard spheres to yield a scaling of the form $D = F(v)d^2\dot{\gamma}$, where d is the particle diameter, $\dot{\gamma}$ is the shear rate, and $F(v)$ is a function of the solid volume fraction (v) (Hajra and Khakhar [22] confirmed the scaling experimentally).

By using the diffusivity as given by Savage [23] ($D = 0.01 R_1^2\dot{\gamma}$), we get t_s written as

$$t_s = \frac{t_D}{\text{Pe}} = \frac{R_1^2}{D\text{Pe}} = \frac{100}{[\beta + (1-c)\alpha](1-c)(1-\bar{d})\dot{\gamma}}, \quad (11)$$

where $\dot{\gamma}$ is the shear rate. This suggests that the critical perturbation frequency, f_c , will vary linearly with the shear rate as

$$f_c = 0.01\dot{\gamma}(1-\bar{d})(1-c)[\beta + (1-c)\alpha]. \quad (12)$$

A simple geometry can be used to illustrate how one might use this critical forcing frequency to “eliminate” segregation as follows. Consider a chute flow that “zigzags” periodically in such a way that, at each bend, the bottom of the previous flow leg now becomes the top of the next flow leg, and so on (see Fig. 1).

If the length, L , of each leg is chosen such that $L < \bar{U}t_s$, our theoretical arguments suggest that segregation can be effectively thwarted. While this simple explanation is theoretically satisfying, physically implementing this model system, either

computational or experimentally, is cumbersome. Specifically, in computations, the radius of curvature of the bend must be tailored *per simulation* in order to not “choke” the flow. Similarly, in the experimental case, the system would need to be prohibitively large (roughly 20 m in height, based on the slow segregation velocities that would be obtained for size ratios close to 1) to reach an asymptotic concentration profile. Instead of using this idealized system, therefore, we instead examine two analogues of the “zigzag” chute that are schematically depicted in Fig. 1 and discussed in detail in the following two sections.

IV. EXPERIMENT

For the experimental analog of the zigzag chute, we perform experiments in hollow square tubes of varying lengths (46, 76, 130, 185, and 246 cm). The flow height of the tube in all cases is approximately 1.8 cm. Tubes are made of transparent polycarbonate. Copper foil tape with conductive adhesive (one end is grounded) is fixed on the backside of the tube to reduce the electrostatic charge of the particles. Silicon carbide screen cloth is attached on the top and bottom surface of the tube to restrict particle slip on the tube surface. Particles are allowed to flow on the surface of the silicon carbide screen cloth only. One end of the tube is open initially and the other end is closed. Once the particles are introduced into the tube, the open end is covered with silicon carbide screen cloth.

Mixtures of monodisperse spherical acetate beads of different diameter (2, 3, 4, and 5 mm) are used. In all experiments, the tube is filled with mixtures composed of 1:1 (v/v) combinations of sizes as described above. The volume of each size of particles in the mixtures is kept constant in all experiments. Tubes are filled with a mixture of each type of bead (individually monodisperse) in such a fashion as to produce an initially mixed condition. That is, we “layer” small volumes of each particle type sequentially in order to form our initial condition. The list of experiments (size combinations) conducted is summarized in Table I.

For each experiment, two trials are performed. In the first case, the tubes are rocked to an angle of roughly 30° —say, to a

TABLE I. Types of binary mixtures used are indicated. For all size ratios, experiments are carried out in five different lengths of tube, i.e., 46, 76, 130, 185, and 246 cm, respectively.

Small particle (mm)	Large particle (mm)	Size ratio (dimensionless)
2	5	0.4
2	4	0.5
3	5	0.6
2	3	0.66
3	4	0.75

right-leaning configuration—in order to induce flow from left-to-right down the inclined plane. Once the flow has stopped, the tube is rotated 180° about its long axis in order to change the orientation of the particles (relative to gravity) prior to the next rocking event [Fig. 1(c)], where the tube will be inclined in a left-leaning sense and so on. We call this a “rock and rotate” experiment. To ensure that there is no movement of particles during rotation of the tube, after the initial particle flow, the tubes are inclined even further (to an angle of inclination > angle of repose) prior to the rotation step (no particle flow occurs during this step). This process is repeated until the particle distribution no longer changes with time. In the second case, the tubes are only rocked and the step involving rotation of the tube is omitted. We call this a “control” experiment.

Photographs are captured after completion of each rocking step for both “rock and rotate” and “control” trials. Two digital cameras (Nikon D200) are used to capture left-leaning and right-leaning images, respectively. The digitized images are used to assess the extent of mixing in both trials. For a quantitative comparison of the extent of mixing, the intensity of segregation (I_s) is calculated via image analysis, using the expression

$$I_s = \left[\frac{\sum_{i=1}^N (C - C_{\text{avg}})^2}{N - 1} \right]^{1/2}, \quad (13)$$

where N is the number of useful cells, C is the concentration of color pixels in a designated cell, and C_{avg} is the average concentration of color pixels in the entire image. We should note that, in each experimental image, we confirm both quantitatively and qualitatively that the pixel measurements accurately reflect the system. Quantitatively, we compare the fraction of pixels identified as each color to the expected input concentration while, qualitatively, we compare segregation patterns between the “raw” and analyzed images.

V. DEM SIMULATION

Particle dynamics, a discrete method of simulation, captures the macroscopic behavior of a particulate system via calculation of the linear and angular motion of each of the individual particles within the mass; the time evolution of these trajectories then determines the global flow of the granular material. The equations that describe the particle motion, therefore, are:

Linear motion:

$$m_p \frac{dv_p}{dt} = -m_p g + F_n + F_t; \quad (14)$$

Angular motion:

$$I_p \frac{d\omega_p}{dt} = F_t \times R, \quad (15)$$

where F_n and F_t are the interparticle forces—normal and tangential, respectively—acting on the particle. The particle trajectories are obtained via explicit solution of Newton’s equations of motion for every particle [24]. The forces and torques on the particles—aside from the effects of gravity—typically are determined from contact mechanics considerations [25]. In their simplest form, these relations include normal (often, Hertzian) repulsion and some approximation of tangential friction (due to Mindlin [26]). A thorough description of possible interaction laws can be found in Refs. [27,28].

Computationally, we mimic the “zigzag” chute using a vertically bounded, periodic box whose sense of gravity oscillates vertically [Fig. 1(a)]. In these 3D simulations, particles are initially randomly mixed, gravity is inclined at angles ranging from 22°–26° with respect to the horizontal, and (frozen) particle-roughened walls are used. Two particle bed heights, 10 and 20 particle diameters, and two size ratios, $\bar{d} = 0.66$ and 0.75, are used in the simulations. In order to simplify the analysis of our results, we examine only those chute simulations that result in both a nonaccelerating asymptotic flow and have a steady velocity profile that is reasonably approximated as being linear (so that extracting an average value for the shear rate is meaningful and the comparison with model predictions is simplified). Our experiments use cellulose acetate particles; however, in our simulations the particle stiffness and other parameters used are reduced in order to decrease the required simulation time (using so-called “soft” particles; a practice shown to have essentially no impact on flow kinematics [29]). Table II lists the material properties used in the simulations.

VI. RESULTS AND DISCUSSION

In our related paper that included theory for density segregation [13], we defined an experiment as yielding a mixed result if the equilibrium I_s value calculated from the “rock and rotate” trial differed (was smaller than) that of the “control” trial. This strategy was (and is) used in order to eliminate any variation in mixing rates within this apparatus that might arise from differences in the flow lengths as we increase the tube sizes. That is, the absolute value of the I_s was not considered

TABLE II. Material properties used in the simulations.

Parameter	Value
Young’s modulus (E , GPa)	0.03
Density (ρ , kg/m ³)	1000
Coefficient of friction (μ)	0.30
Poisson ratio (ν)	0.33
Yield stress (σ_y , MPa)	0.3

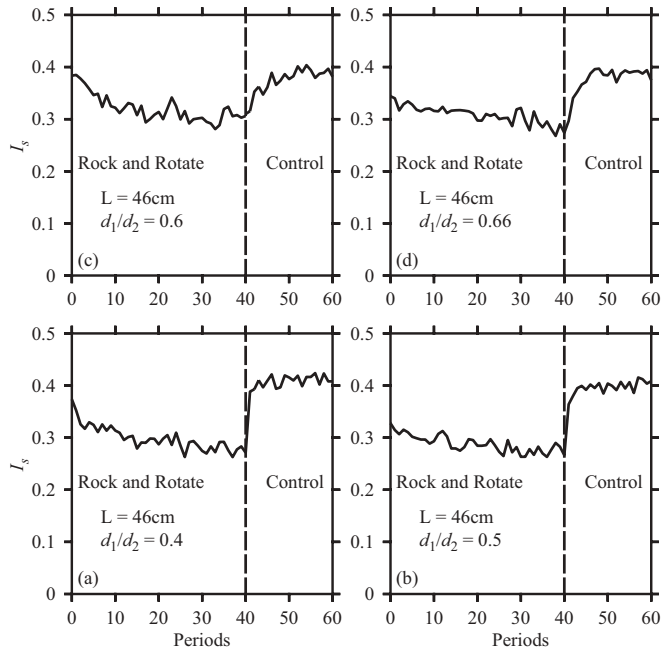


FIG. 2. The intensity of segregation as a function of time for a variety of particle size combinations for a tube length of $L = 46$ cm. In each case, there is a clear step change between the I_s values between the “rock and rotate” and “control” regions of the experiments. In all cases, we consider this to yield a mixing result.

to be significant, but the *change* in that value between the rock and rotate versus the control was used as a discriminator.

In the current work, focused on size segregation, this technique for analyzing the experimental results of the rock-and-rotate apparatus works well for the “extreme” cases. For example, Fig. 2 shows the I_s profiles for various size ratio combinations that yield results from the “rock and rotate” trial that are substantially smaller than that of the “control” trial. In other words, there is a clear step change (upward) in the value of I_s when we begin the control trials in each case shown, so all of these size ratios are considered to yield a mixing result for this tube length ($L = 46$ cm). Similarly, Fig. 3 shows the I_s profiles for various size ratio combinations where there is no discernible difference in the equilibrium values of I_s for the “rock and rotate” versus the “control” trial. For this tube length ($L = 246$ cm), all of these size ratios are considered to yield a segregating result.

In contrast to the density segregation case, for size segregation trials near the mixing and segregation boundary, determining the proper interpretation of our experimental outcome is more difficult. This is due, in part, to the fact that these more strongly segregating materials (note that size segregation is typically considered to be a dominant mode when compared to density segregation) lead to segregation in the direction parallel as well as perpendicular to the flow. This difficulty is also due to the fact that size segregation is strongly affected by the presence of boundaries so that our experimental results (which rely on boundary images) need to be interpreted with an eye toward “wall segregation” as well. Thus, an additional quantitative discriminator is used in assigning results as either mixed or segregated. That is, we compare the rock-and-rotate results from the “right-leaning”

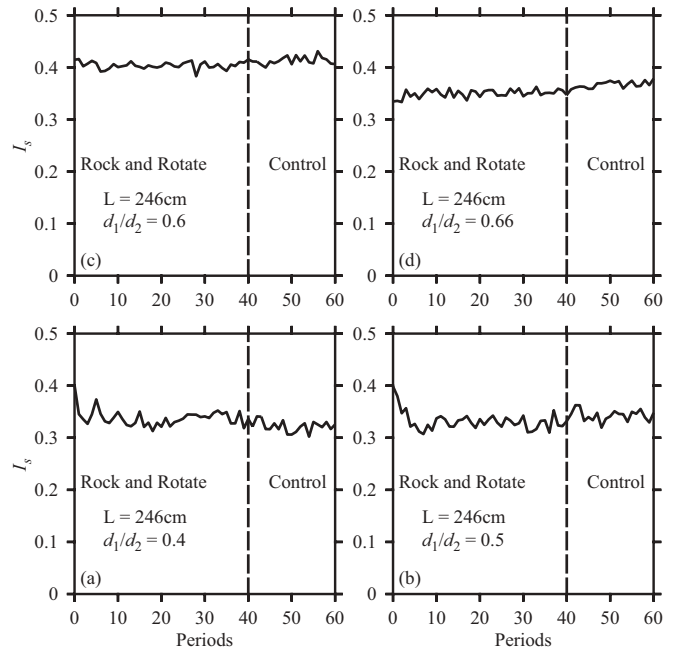


FIG. 3. The intensity of segregation as a function of time for a variety of particle size combinations for a tube length of $L = 246$ cm. In each case, there is no discernible difference in the I_s values between the “rock-and-rotate” and “control” regions of the experiments. In all cases, we consider this to yield a segregating result.

rock to those from the “left-leaning” rock. If we consider the two relevant time scales, the segregation time (t_s) and the flow time ($t_f = L/\bar{U}$), we have three possible scenarios: $t_s \ll t_f$, $t_f \gg t_s$, and $t_s \approx t_f$. Interestingly, if the time scales are vastly different both the right- and left-leaning rock results will be the same. This is because the system either had more than enough time to segregate in both halves of the rock cycle, or it had far too little time to segregate in either case. In contrast, when we are close to the mixing and segregation boundary, $t_s \approx t_f$, so that our materials may segregate somewhat on the right-leaning rock (which started out mixed), but the left-leaning rock has only enough time to “undo” that segregation. It does not have enough time to segregate in the opposite sense. This leads to the I_s profiles for the right-leaning and left-leaning results that are internally consistent for either a mixed or a segregated result, but differ (from each other) when we are near the mixing and segregation boundary. Figure 4 shows I_s profiles for a size ratio of 0.6 for a mixed result (a), a “boundary” result (b), and a segregated result (c). Note that the system we consider mixed (a) and segregated (c) both have strong similarity between the “left-leaning” (solid) and “right-leaning” (dashed) results, while the “border” case shows a discrepancy between left and right results. Here, we consider the right result (c) to be segregated since the “left-leaning” (solid) and “right-leaning” (dashed) results are similar and indistinguishable from the “control” portion. In contrast, the result that is considered “mixed” (a) has similar “left-leaning” (solid) and “right-leaning” (dashed) results, but control portions of the experiment that differ from each other as the system alternatively mixes then segregates (somewhat) is each leg of the control (for this rather long chute, there

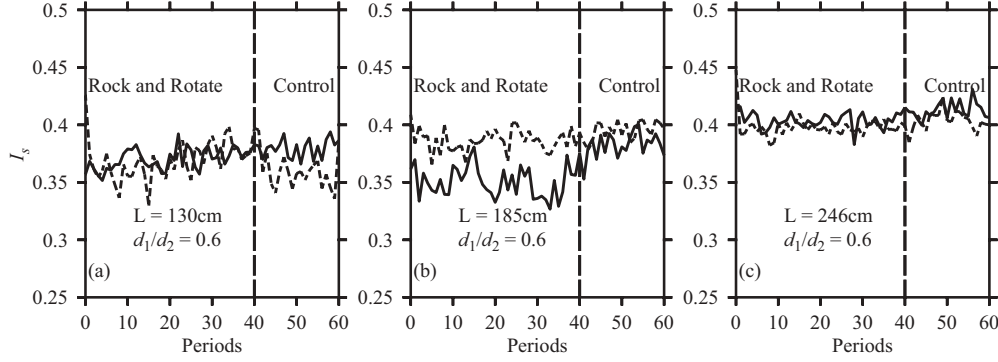


FIG. 4. The intensity of segregation with times for the transition zone (mixed to segregated result) for “rock-and-rotate” and “control” experiments for three different tube lengths for a size ratio of 0.6. The solid lines represent the results for the left-leaning images, while the dashed line is for the right-leaning images. Note that the system we consider mixed (a) and segregated (c) both have strong similarity between the left- and right-leaning results, while the “border” case shows a discrepancy between left and right results.

is substantial segregation in the flow direction once vertical segregation is allowed to take place).

VII. MODEL PREDICTIONS

As discussed previously, we test our model by comparing our predictions against both simulations in our infinite chute flow as well as in our “rock-and-rotate” experiments. In both cases, we have two fitted parameters— β and α —and a host of trivially measured quantities [such as the tube height and length, the initial (input) concentration of particles, the particle size ratio, etc.].

Examining first our “flipped” infinite chute flows, we empirically fit $\beta = 0.2$ and $\alpha = 3.5$ (and recall that our initial, input concentration is $c = 0.5$), so that Eq. (12), along with a computationally measured shear rate for each simulation, yields a prediction of the critical forcing frequency. We plot the results of our simulations as a function of the ratio of the gravitational “flipping” frequency to the calculated value of f_c . Here, since we allow the system to reach an asymptotic state, the magnitude of the intensity of segregation (I_s) is a

valid measure of the mixedness and we consider high values (typically greater than 0.25) to imply a poorly mixed system while low values correspond to good mixing. This suggests that the plot of our simulation results in Fig. 5(b) should yield points with high values of I_s for $f/f_c < 1$ and low values of I_s when $f/f_c > 1$. The results of a number of “zigzag” simulations of size segregation—with varying conditions as described above—are shown in Fig. 5(a). We should note that, although the results for a size ratio of 0.66 agree with our predictions, the results for 0.75 are somewhat at odds. The trend of an inverse relationship between I_s and f/f_c is seen, but the small values of f/f_c do not lead to a segregated system (perhaps due to the fact that the segregation driving force for such a high size ratio is negated by the diffusive mixing inherent in the relatively high energy chute flow).

Analyzing the results of the experiments, one notes that the ratio f/f_c is a function of the size ratio and aspect ratio of the tube only. That is, there is no need to measure either the flow velocity or the shear rate. This can be understood as follows. We first verified [13] that the flow down the inclined plane is essentially linear (using metallic particles and “streak line” measurements [14]). This suggests that the shear rate can be simply expressed as $\dot{\gamma} = 2\bar{U}/H$, where \bar{U} is the average streamwise flow velocity and H is the radial height of the rod. We then note that the effective forcing frequency is given as

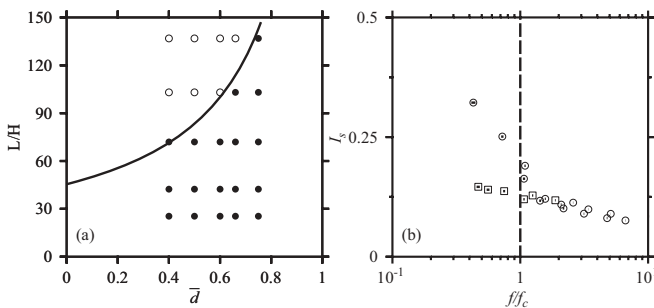


FIG. 5. Shown is a comparison of our results with the theoretical predictions. On the left (a) we summarize the experimental results from the rock-and-rotate “chute”. Plotting our experimental results as a function of tube aspect ratio versus size ratio, we obtain agreement with theory [Eq. (16)] with $\beta = 0.2$, $\alpha = 4$, and $c = 0.5$ —the solid circles denote mixed systems, and the open circles denote segregated systems. On the right (b), we show computational results where high (low) values of I_s are found when f/f_c is less (greater) than 1. We use circles to denote a size ratio of 0.66 and squares for 0.75.

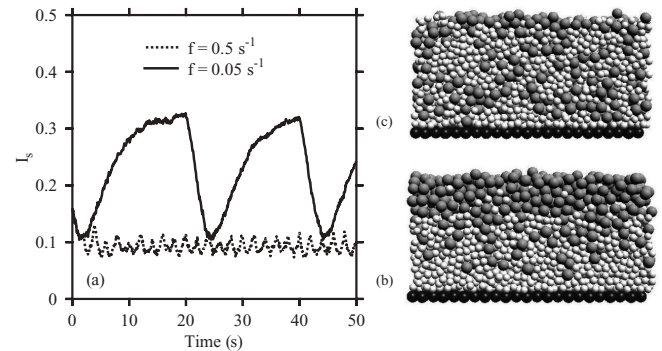


FIG. 6. Shown are representative computational results for both a mixed (c) and segregating (b) system. The left side (a) shows the time-variation of the I_s values corresponding to the inset images.

$f = 2\bar{U}/L$, so that [using Eq. (12)] our values of \bar{U} cancel and we are left with a primarily geometric expression:

$$\frac{f}{f_c} = \frac{100H}{[\beta + (1-c)\alpha]L(1-c)(1-\bar{d})}. \quad (16)$$

Fitting our β and α values to the results obtained at the size ratio $\bar{d} = 0.6$, we obtain $\beta = 0.2$ and $\alpha = 4$. We then plot the results of all of the experiments with mixtures of different-sized cellulose acetate beads in Fig. 5(a). We note that, as predicted, the categorization of the system as either mixed or segregated agrees with the boundary curve suggested by Eq. (16) (using the fitting parameters from the the size ratio of 0.6 only, as this one included our “boundary” case as seen in Fig. 4).

Finally, in Fig. 6 we depict representative results for mixing and segregation trials of the computational zigzag chute. On the left we show the time evolution of the I_s values for the duration of the simulations. Note that the segregating system exhibits a time-periodic tracing of the I_s and the system must reverse the sense of segregation after each “flipping” event. This means that after each “flipping” event the system passes through an unstable “mixed” configuration on its way to the new segregated state (much like what is exhibited in the discrepancy between the right-leaning and left-leaning rock-and-rotate systems that are close to $t_s = t_f$). On the right (b and c) we show a snapshot of the left-hand systems with the segregating system at the bottom (b) and the mixed system at the top (c).

VIII. CONCLUSION

In this work we apply flow perturbations in order to eliminate segregation due to size differences (S systems) in surface-dominated granular flows. We develop an approximate theory applicable to S systems that is analogous to that developed by Shi *et al.* [13] for D systems and show that it matches both computational results in a chute flow and experimental results in a “rock-and-rotate” tube. Experimentally, a mixed result is obtained for all size ratios when a short length of tube is used; however, a segregated result is obtained for a sufficiently long length of tube. Adapting our approximate theory to this simple geometry allows us to develop a model for the critical perturbation frequency that is only a function of size ratio and tube aspect ratio. Thus, by controlled duration of chute flow lengths, one might limit free surface segregation in a simple way. This work could be extended for combined size and density coupled mixtures, where particles are completely segregated due to combined effects of “void-filling” and “effective buoyancy” mechanisms. Finally, this concept of time modulation could be applied for a wide range of industries, where the finished product strictly depends on the quality of mixing of the bed materials, such as pharmaceuticals, food stuffs, ceramics, etc.

ACKNOWLEDGMENT

We are grateful for the financial support for this work from the National Science Foundation, Grant No. CBET-0933358.

-
- [1] J. B. Knight, H. M. Jaeger, and S. R. Nagel, *Phys. Rev. Lett.* **70**, 3728 (1993).
 - [2] J. Gray and K. Hutter, *Continuum Mech. Thermodyn.* **9**, 341 (1997).
 - [3] H. A. Makse, S. Havlin, P. R. King, and H. E. Stanley, *Nature (London)* **386**, 379 (1997).
 - [4] A. Samadani and A. Kudrolli, *Phys. Rev. Lett.* **85**, 5102 (2000).
 - [5] A. Samadani, A. Pradhan, and A. Kudrolli, *Phys. Rev. E* **60**, 7203 (1999).
 - [6] O. Zik, D. Levine, S. Lipson, S. Shtrikman, and J. Stavans, *Phys. Rev. Lett.* **73**, 644 (1994).
 - [7] K. M. Hill, A. Caprihan, and J. Kakalios, *Phys. Rev. Lett.* **78**, 50 (1997).
 - [8] D. Khakhar, A. Orpe, and S. Hajra, *Physica A: Stat. Mech. Appl.* **318**, 129 (2003).
 - [9] H. Li and J. J. McCarthy, *Phys. Rev. Lett.* **90**, 184301 (2003).
 - [10] N. Jain, J. M. Ottino, and R. M. Lueptow, *Granular Matter* **7**, 69 (2005).
 - [11] N. Thomas, *Phys. Rev. E* **62**, 961 (2000).
 - [12] S. K. Hajra and D. V. Khakhar, *Improved Tumbling Mixers and Rotary Kilns* (Indian Patent No. 213856, 2003).
 - [13] D. Shi, A. A. Abatan, W. L. Vargas, and J. J. McCarthy, *Phys. Rev. Lett.* **99**, 148001 (2007).
 - [14] D. V. Khakhar, J. J. McCarthy, and J. M. Ottino, *Phys. Fluids* **9**, 3600 (1997).
 - [15] V. Dolgunin, *Powder Technol.* **83**, 95 (1995).
 - [16] J. T. Jenkins and F. Mancini, *Phys. Fluids A* **1**, 2050 (1989).
 - [17] S. Hsiau and M. Hunt, *Acta Mech.* **114**, 121 (1996).
 - [18] Y. Fan and K. M. Hill, *Phys. Rev. E* **81**, 041303 (2010).
 - [19] S. B. Savage and C. K. Lun, *J. Fluid Mech.* **189**, 311 (1988).
 - [20] V. Dolgunin, A. Kudy, and A. Ukolov, *Powder Technol.* **96**, 211 (1998).
 - [21] S. Savage and R. Dai, *Mech. Mater.* **16**, 225 (1993).
 - [22] S. K. Hajra and D. V. Khakhar, *Phys. Fluids* **17**, 013101 (2005).
 - [23] S. B. Savage, in *Disorder and Granular Media*, edited by D. Bideau and A. Hansen (Elsevier Science, Amsterdam, 1993), pp. 255–285.
 - [24] P. A. Cundall and O. D. L. Strack, *Géotechnique* **29**, 47 (1979).
 - [25] K. L. Johnson, *Contact Mechanics* (Cambridge University Press, Cambridge, 1987).
 - [26] R. D. Mindlin and H. Deresiewicz, *J. Appl. Mech.* **20**, 327 (1953).
 - [27] J. J. McCarthy and J. M. Ottino, *Powder Technol.* **97**, 91 (1998).
 - [28] J. J. McCarthy, V. Jasti, M. Marinack, and C. F. Higgs, *Powder Technol.* **203**, 70 (2010).
 - [29] O. Walton, *Int. J. Eng. Sci.* **22**, 1097 (1984).